WATER RESOURCES RESEARCH, VOL. 32, NO. 12, PAGES 3553–3570, DECEMBER 1996

Contributions of water-rock interactions to the composition of groundwater in areas with a sizeable anthropogenic input: A case study of the waters of the Fundão area, central Portugal

Fernando Pacheco

Secção de Geologia, Universidade de Trás-os-Montes e Alto Douro, Vila Real, Portugal

Cornelis H. van der Weijden

Department of Geochemistry, Institute of Earth Sciences, Utrecht University, Utrecht, Netherlands

Abstract. We used a combination of a grouping algorithm and a weathering algorithm to assess the contributions made by chemical weathering and anthropogenic inputs to the groundwater composition in a granitoid area. The first algorithm is based on the mathematical concept of equivalent relations between objects and is used to find groups of water samples. Using the grouping algorithm, we identified groups with similar chemistries in a set of data relating to the water composition in 160 springs and wells in the Fundão area (Portugal). The second algorithm is based on stoichiometries, mass, and charge balances in weathering reactions and is used to relate the water composition of each identified group to water-mineral interactions in the area. Background information on the petrology and mineralogy of the area allowed us to choose the most realistic water-mineral interactions. We also had information about the use and composition of fertilizers in this agricultural area. In applying the weathering algorithm we considered all dissolved silica and bicarbonate to be produced by chemical weathering and all dissolved chloride, sulphate, and nitrate to be derived from other sources, mainly from fertilizers. The anthropogenic contributions to the water chemistries in the area are high. Despite the high background concentrations derived from pollution, we were able to assess the contribution of weathering to the water chemistries. We obtained realistic results with the two algorithms, supported by the fact that the spatial distribution of the samples belonging to the various groups shows a good correlation with the geology and petrology of the area.

Introduction

The composition of natural waters is determined by a number of processes, which include wet and dry deposition of atmospheric salts, evapotranspiration, and water-soil and water-rock interactions. *Garrels and Mackenzie* [1967] presented a classical analysis of the natural processes responsible for the composition of springs and groundwater in a pristine area. First, they corrected the water composition for atmospheric input and then, step by step, they used the cations, anions, and dissolved silica to reconstruct the primary minerals from their secondary weathering products until all dissolved components had been used. From the stoichiometry of these reverse weathering reactions they estimated the mass of the primary minerals involved in the water-rock interactions. Quite a number of studies on the relation between groundwater composition and water-rock interaction have been carried out since then. We refer to work published by *Garrels* [1967], *Tardy* [1971], *Tardy et al.* [1973], *Pačes* [1971, 1973], *Drever* [1988], *Sverdrup and Warfvinge* [1991], and *Velbel* [1985a, b, 1989, 1992] and references therein. These studies were carried out in areas with a minimum anthropogenic input. Such areas are becoming increasingly scarce, and in many areas the groundwater contains a considerable amount of chemicals derived from human activities.

In inhabited areas, especially where there is intensive agriculture and/or industry, the water composition is usually affected by fertilization and manuring, by leachates of solid waste, and by domestic and industrial effluents. In general, there is no easy way to distinguish between the contributions made by natural sources and those made by anthropogenic sources. The only components that in all likelihood, are solely or at least predominantly derived from water-rock interactions are silica and bicarbonate. In this paper we will discuss the results of a method that combines a mathematical algorithm (based on the concept of equivalent relations) that can identify groups in a set of groundwater analyses and a weathering algorithm that relates the group medians to water-mineral interactions. The water samples were collected in the Fundão area (Portugal), situated in a granitoid complex intersected by a number of aplites and basic dikes.

The Fundão Area

The Fundão area (Figures 1a and 1b) is situated in the province of Beira Baixa (central Portugal). The area is located at the confluence of the Zêzere and Meimoa rivers. The lowest part of the area lies about 400 m above sea level. The Serra da

Paper number 96WR01683.
0043-1397/96/96WR-01683$09.00

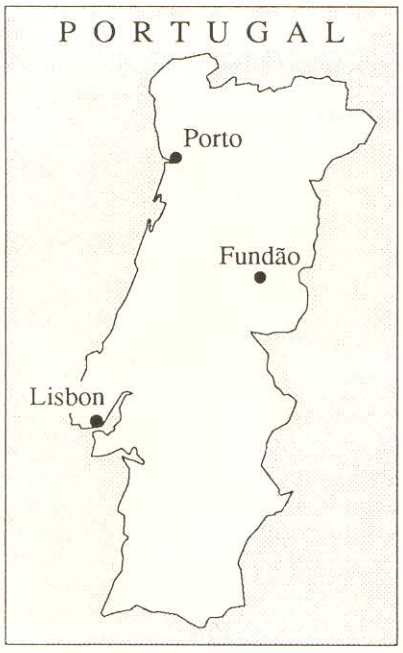

Figure 1a. Geographical map of Portugal indicating the position of the Fundão area.

Gardunha, bordering the area in the south, has peaks between 1200 and 1300 m above sea level. Hills bordering the area to the east and west have altitudes of between 500 and 600 m. This leads to a general drainage pattern in the NW direction, but the drainage pattern is also controlled by the SSW-NNE direction of faults in this region. The streamlets are intersected by the Rio da Meimoa, which crosses the area from east to west just south of Alcaria. The streamlets from the Serra da Gardunha are perennial, but upon reaching the valley most of their water disappears into the weathered granitoid subsoil. During summer, water is transported mainly through streambed gravels.

The groundwater flow in the area depends on the topography of the contact between fresh and weathered rocks. The system of joints does not have a large storage capacity. The area, more specifically the southern part, has many springs, most of them perennial. Many wells have been dug in the area, mainly in the valley. The wells that are close to the streambeds give large yields, but farther from the beds the yields are small (a few cubic meters per day).

The climate is very good for agriculture; this is concentrated in the southern part, where there is a plentiful water supply. The poor granitic soil has to be fertilized. Besides the nutrients nitrate, ammonium, phosphate, and potassium, the locally applied fertilizers also contain high amounts of calcium, chloride, and sulphate and minor amounts of sodium. Fertilizers high in magnesium are also frequently applied in apple and cherry orchards in the area. The fertilization has a large impact on the water chemistry. As a first-order working hypothesis, we assume that the application of fertilizers has resulted in a steady state occupancy of exchange sites by the major cations. The atmospheric input of carbonate particles is negligible and liming of the soils in the area is only sporadic. Therefore one is justified in assuming that all bicarbonate is derived from water-rock interaction.

Petrology and Mineralogy

Petrology

The Fundão plutonite has an exposed area of approximately 100 km^2. The main lithological types present (Figure 2a) are tonalites, although some granites and monzonitic granites appear in places. These units are cut by two dominant types of

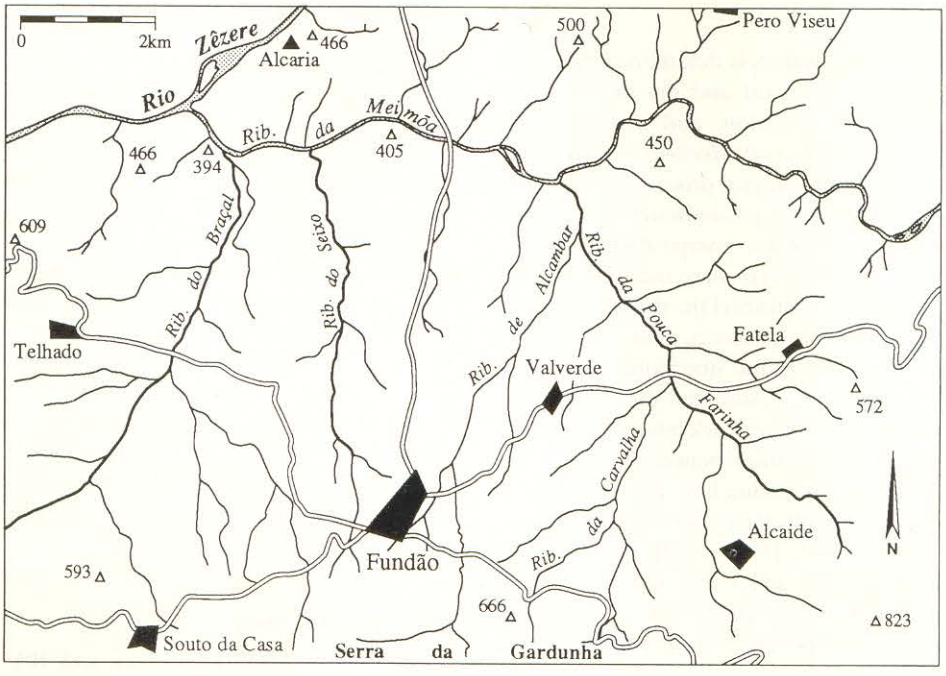

Figure 1b. Blow-up of the Fundão area with the major villages (black polygons) and connecting roads (double lines), the rivers Zèzere and Meimoa and their tributary streams and streamlets, topographical heights (triangles with altitudes in meters above sea level), and the position of the Serra da Gardunha.

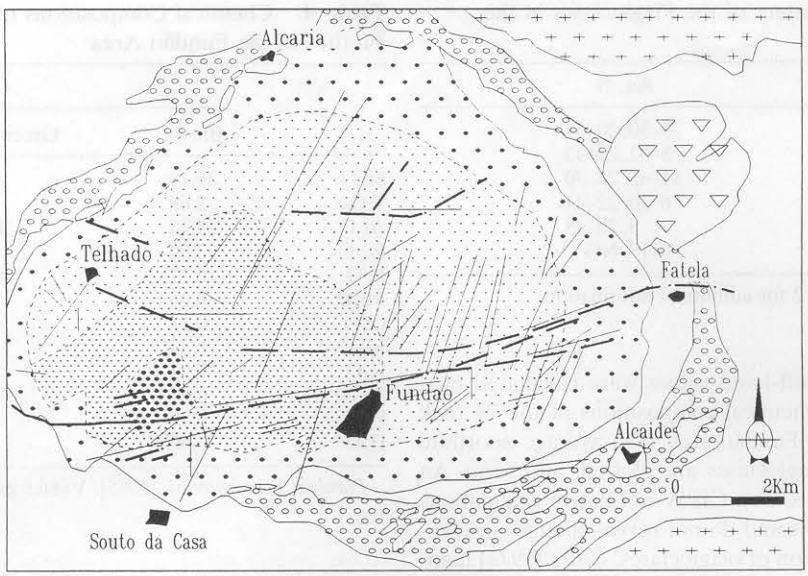

Legend:

- γ_5 - Monzonitic granite
- Δ_0 - Tonalite
- Δ_1 - Granodiorite
- Δ_2 - Biotitic tonalite
- $\gamma\Delta_3$ - Biotitic-monzonitic granite
- γ_6 - Porfiroid-biotitic granite
- γ_8 - Muscovitic-albitic granite
- Hornfelses and micaschists
- Basic rocks
- Fractures

Figure 2a. Geological map of the Fundão area (simplified and modified after *Portugal Ferreira et al.* [1985]).

structures: (1) EW alignments, consisting in a dike swarm of basic and in some cases aplitic rocks, and (2) N35E faults, filled with breccias and showing strong evidence of hydrothermal alterations [*Portugal Ferreira et al.*, 1985]. The chemical compositions of the distinct petrographical units (Figure 2a) are depicted in Table 1. The basic dikes are amphibolites, metadiabases, and diabases.

Table 1. Average Chemical Compositions of the Petrographical Units in the Fundão Area Shown in Figure 2a

	Δ_0	Δ_1	Δ_2	$\gamma\Delta_3$	γ_5	γ_8
SiO_2	67.0	65.2	65.1	70.4	75.9	73.0
TiO_2	0.51	0.58	0.52	0.33	0.07	0.16
Al_2O_3	15.8	16.6	16.5	15.5	14.0	14.9
Fe_2O_3	1.23	1.21	1.22	0.75	0.88	0.49
FeO	2.29	2.56	2.36	1.41	1.30	0.81
MnO	0.06	0.06	0.05	0.03	0.01	0.03
CaO	3.17	3.00	3.17	1.39	0.02	0.50
MgO	1.47	1.76	1.74	0.84	0.29	0.25
K_2O	2.21	3.14	2.73	3.55	4.63	4.34
Na_2O	4.40	3.76	4.29	3.67	0.37	3.57
P_2O_5	0.21	0.27	0.25	0.22	0.11	0.40
LOI	1.40	1.41	1.55	1.84	2.01	1.26
Total	99.8	99.6	99.5	99.9	99.6	99.7
n	12	20	19	9	3	11

Values given in percent; *n*, number of samples.

Mineralogy

The mineralogical compositions of the granitoid units are given in Tables 2 and 3. For each mineral the right-hand values were determined by mean modal analyses [*Portugal Ferreira et*

Table 2. Average Mineralogical Compositions of the Grantoid Units in the Fundão Area

Lithotype	Quartz	Plagioclase	K-spar	Biotite	Muscovite
Δ_0	23, 30	52, 50	14, 3	11, 16	···
Δ_1	21, 30	49, 41	18, 12	12, 16	···
Δ_2	23, 31	48, 45	16, 7	13, 17	···
$\gamma\Delta_3$	31, 36	36, 29	21, 25	12, 10	···
γ_5	50, 33	13, 36	26, 18	2, 2	9, 11
γ_8	35, NG	30, NG	26, NG	2, NG	8, NG

Values in weight percent. Cf. Figure 2a. The right-hand values under each mineral name was calculated by *Portugal Ferreira et al.* [1985] using mean modal analysis; the left-hand values in each column were obtained from normative calculations (CIPW norm) using the chemical compositions given in Table 1. NG, not given by *Portugal Ferreira et al.* [1985].

Table 3. Anorthite Content of the Plagioclases in the Various Grantoid Units

Lithotype	An, %
Δ_0	25–30, 20–33
Δ_1	8–32, 20–33
Δ_2	11–45, 24–30
$\gamma\Delta_3$	6–20, 22–44
γ_5	0, 20–45
γ_8	0–17, NG

Cf. Figure 2a. See Table 2 for additional information.

Table 4. Chemical Compositions of Three Representative Biotites in the Fundão Area

	Color		
	Brown	Green to Brown	Green
SiO_2	36.78	27.39	37.96
TiO_2	2.68	2.66	2.98
Al_2O_3	15.75	16.19	15.01
Fe_2O_3	3.90	3.15	4.58
FeO	16.77	16.86	14.91
MnO	0.26	0.27	0.28
CaO	0.11	0.14	0.05
MgO	8.34	8.76	8.96
K_2O	9.93	9.04	9.67
Na_2O	0.69	0.84	0.75
P_2O_5	0.29	0.30	0.26
H_2O^+	3.60	3.12	3.16

Portugal Ferreira et al. [1985]. Values given in percent.

al., 1985], whereas the left-hand values were calculated by a CIPW norm using the chemical compositions of the 74 rock samples collected in the Fundão area. The average anorthite (An) contents of the plagioclases are plotted, and some An isolines are drawn (Figure 2b). CIPW normative calculations give average compositions and do not reveal changes in composition related to zonation of plagioclases. *Costa* [1971] mentions that in the γ_5 and $\gamma\Delta_3$ granitoids plagioclase has a homogeneous composition (An 10 and An 20, respectively), whereas in the central plutonite (Δ_{0-2}) the plagioclases are strongly zonated (the composition of single minerals may vary in composition from An 18 to An 37). The composition of the biotites is shown in Table 4. The basic dikes are characterized by the major minerals [*Portugal Ferreira*, 1982]: amphibolites: hornblende, andesine (An 40–50); metadiabases: hornblende, andesine (An 40–50); and diabases: augite, labradorite (An 50–70). The composition of aplitic dikes in the area was determined by *Costa et al.* [1971]. In addition to the more weathering-resistant minerals quartz, potassium feldspar, and muscovite, these aplites contain albite or sodic oligoclase and biotite.

Soils

The soils in the Fundão area have a homogeneous mineralogical composition, defined by the association quartz + feldspar + biotite + halloysite, with small amounts of smectite, vermiculite, chlorite, and muscovite [*Costa et al.*, 1971]. During the weathering of the rocks, biotite may have been altered to vermiculite, smectite, or even halloysite, and plagioclase to halloysite. The southeastern part of the plutonite is more deeply weathered than the northwestern part, probably because the southeastern part of the plutonite is covered by torrential deposits from the Serra da Gardunha. Furthermore, the $\gamma\Delta_3$ granite has been very intensively weathered, because this unit is clenched between the more consistent schist rings that have often been metamorphozed to hornfelses [*Van der Weijden et al.*, 1983].

Water-Rock Interactions

Not all the minerals present in the various rocks of the plutonite are important as weathering reactants. The weathering products are mainly derived from plagioclase and biotite. Different degrees of weathering are found in different parts of the Fundão area: the SE part is more deeply affected than the

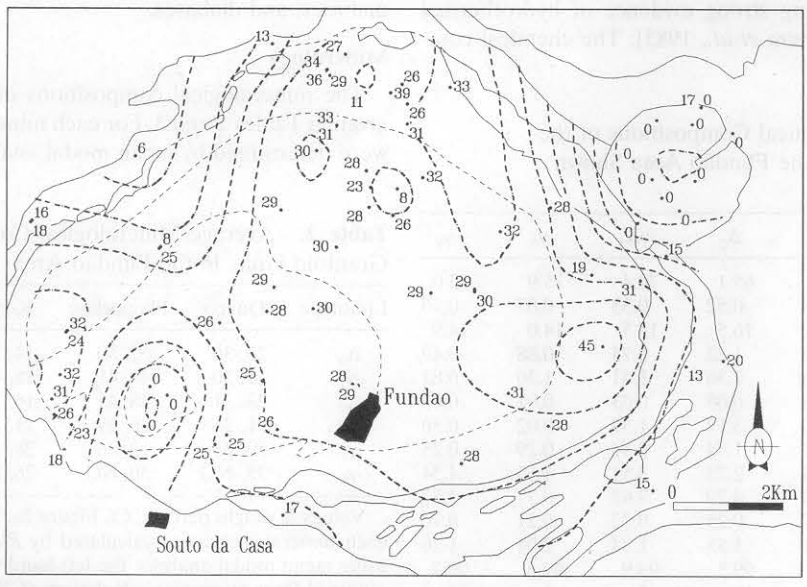

Figure 2b. Contours of iso-anorthite contents (5% increments) of plagioclases, calculated on the basis of analyses of 74 rock samples collected in the Fundão area.

Table 5a. Assumed Weathering Model for the Plutonite

Major Primary Minerals	Weathering Products/Processes		
	Light	Moderate	Intensive
Plagioclase			
Plutonite*	a	a	a
Faults†	b	b	b
Biotite			
Plutonite*	c	d	d
Faults†	e	e	e

Plagioclase: An 7 for γ_5 and γ_8; An 20 for $\gamma\Delta_3$; An 20–40 for Δ_{0-2}. Here a, halloysite; b, (c_1) Ca-montmorillonite + $(1 - c_1)$ halloysite; c, unweathered; d, (c_1) vermiculite + $(1 - c_1)$ halloysite; e, (c_1) vermiculite + $(1 - c_1)$ halloysite; $0 \leq c_1 \leq 1$.

*Relatively good drainage conditions.

†More stagnant conditions.

Table 5b. Assumed Weathering Model for the Dikes

Rock Type	Weathering Reactions of the Major Minerals
Aplites	albite → halloysite
Amphibolites and metadiabases	andesine → (c_1) MgCa-montmorillonite + $(1 - c_1)$ halloysite
	hornblende → (c_1) MgCa-montmorillonite + $(1 - c_1)$ chlorite
Diabases	labradorite → (c_1) MgCa-montmorillonite + $(1 - c_1)$ halloysite
	augite → (c_1) MgCa-montmorillonite + $(1 - c_1)$ chlorite

Plagioclase: An 7 for the aplites, An 40 for the amphibolites and metadiabases, and An 60 for the diabases; $0 \leq c_1 \leq 1$.

NW, and the $\gamma\Delta_3$ granite has been intensively weathered. The N35E fault system may also control the water chemistry by creating more stagnant conditions of flow. These aspects are considered in Table 5a. A similar dominance of reactions was taken into account by *Tardy et al.* [1973] for the weathering of granites in temperate climates. Where dikes cross the plutonite they may also control the water chemistry. The most probable alteration processes that occur in the aplitic and basic dikes are represented in Table 5b.

Sampling and Analysis

Samples from springs and wells in the Fundão area were collected for several years in succession. The locations of 160 sampling sites are shown in Figure 3. The analytical methods that were used have been described by *Van der Weijden et al.* [1983]. These methods will be briefly summarized here. Conductance (Ec) and *p*H were measured immediately at the sampling site. In a field laboratory alkalinity was determined, using the Gran plot method, within 24 hours after collecting the samples.

In the home laboratory sodium, potassium, magnesium, and calcium were determined by routine atomic absorption (AAS) or inductively coupled plasma spectrometry (ICP-AES). The sulphate concentration was determined by turbidimetry or by ICP-AES. The phosphate, silica, and nitrate concentrations were determined by colorimetry. House standards were used for calibration. The relative standard deviations for the individual concentrations were in most cases less than 5%. The deviation of the charge balance was less than 10% of the total ionic charge. As one might expect, the higher relative deviations within this range were usually found for samples with low concentrations of dissolved components.

Grouping Water Samples With Similar Chemistries: The RST Algorithm

Partitioning Methods

Conventional partitioning methods [cf. *Hartigan*, 1975; *Everitt*, 1977] construct clusters from a data set. The number of clusters, k, is given by the user, and each object must belong to one group only. In order to obtain the k clusters, some methods select k representative objects in the data set, and the corresponding clusters are then found by assigning each remaining object to the nearest representative object. Fuzzy methods also construct k clusters, but they avoid hard deci-

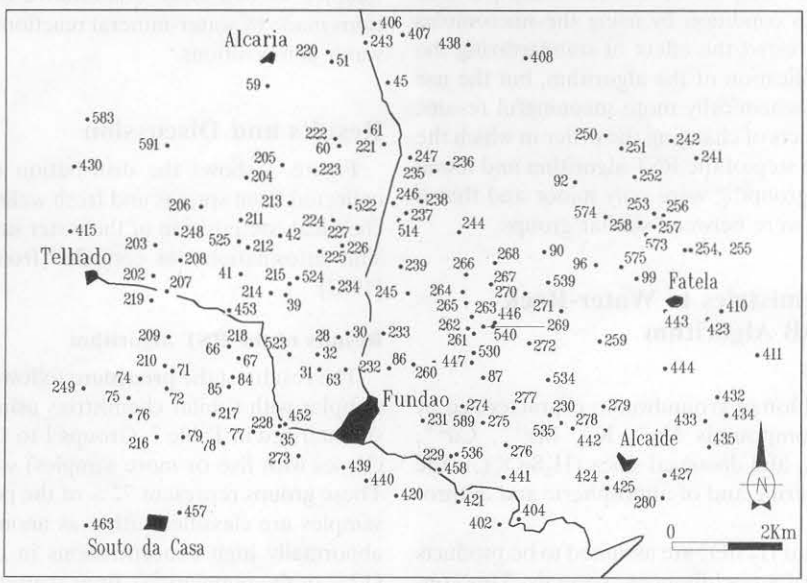

Figure 3. Distribution of the 160 spring and well water samples collected in the Fundão area.

sions by using the fuzziness principle. Instead of deciding that an object belongs to cluster 1, fuzzy methods can, for example, decide that 70% of an object belongs to cluster 1, 20% to cluster 2, and 10% to cluster 3. This means that the object should probably be assigned to cluster 1 but that there is still doubt about whether it should be assigned to cluster 2 or 3 [*Kaufman and Rousseeuw*, 1990].

Conventional and fuzzy methods need a priori good estimates of the number of groups present in the data set. This is often impossible when one is dealing with groundwater data sets because the number of groups that are present will depend on (1) the number of rock types in the area, (2) the degree of chemical weathering of various rock types, and (3) inputs from sources other than water-rock interactions. All these factors affect the water composition and in combination may generate a high number of water groups. These clustering methods also assume that the variables measured on each object (water sample) belong to normal or lognormal populations, which in many cases might be a hard assumption.

Partitioning Using the Concept of Equivalent Relations

In order to avoid the drawbacks of the conventional clustering methods, we were in need of a more powerful method to identify water samples with similar chemistries. In mathematical terminology water samples within these groups will have equivalent relations, meaning that they are in the same equivalence class of "sameness" by their chemistries. The reflexive, symmetric, and transitive (RST) algorithm has been developed for finding groups of water samples with similar chemistries in a data set. A full description of the algorithm is given in Appendix 1.

Grouping the Water Samples From the Fundão Data Set

As mentioned in Appendix 1, the results obtained with the RST algorithm depend on the scale in which the data are expressed. We applied the algorithm to the data set in the micromoles per liter and microequivalents per liter scales, but we obtained the most meaningful results using the micrograms per liter scale. The better performance of the latter scale might be due to avoidance of a closed-sum effect by introducing the charge balance condition using the microequivalents per liter scale or approaching this condition by using the micromoles per liter scale. We also tested the effect of standardizing the data set prior to the application of the algorithm, but the use of the raw data gave geochemically more meaningful results. Finally, we tested the effects of changing the order in which the data are used in the third step of the RST algorithm and found that the changes in the grouping were only minor and that if changes occurred, these were between similar groups.

Relating Water Chemistries to Water-Rock Interactions: The SiB Algorithm

Water-Rock Interactions

The chemical composition of groundwater, characterized by the major inorganic compounds Na^+, K^+, Mg^{2+}, Ca^{2+}, HCO_3^-, Cl^-, SO_4^{2-}, NO_3^- and dissolved silica ($H_2SiO_3^o$), is the result of chemical weathering and of atmospheric and anthropogenic inputs.

All dissolved HCO_3^- and $H_2SiO_3^o$ are assumed to be products of chemical weathering of autochthonous minerals. This condition is not met in areas with sizable input of limestone dust or application of calcium carbonate on agricultural land, which, as mentioned already, can be neglected in this area. We also have no indications for secondary precipitation of carbonate or silica. Alkalinity of groundwater may change, either by selective uptake of nitrate in exchange with bicarbonate or by harvesting of crops which have taken up cations in excess over anions from soil water in exchange with protons. For a region with a mixture of agriculture, viniculture, fruit culture, forestry, and uncultivated areas with grasses and scrubs, it is impossible to quantify the net effect of such changes in alkalinity. We assume that in the Fundão region these processes have relatively little effect on the general level of alkalinity acquired by water-rock interactions under soil P_{CO_2}. We also assume that loss of dissolved silica by uptake in harvested crops is negligible. *Garrels* [1967] showed that dissolved HCO_3^- and $H_2SiO_3^o$ and their ratios are good diagnostic parameters for particular water-mineral interactions. As a working hypothesis, dissolved Cl^-, SO_4^{2-} and NO_3^- are considered to come from atmospheric and pollution sources. The presence of pyrite as a potential source of sulphate can be neglected in the area. The concentration of each cation is separated in two partial contributions, one related to the weathering reactions, and the other related to pollution. In order to quantify these partial contributions we developed a weathering algorithm, which we called the SiB (silica-bicarbonate) algorithm. This algorithm is described in detail in Appendix 2.

Relating Water Compositions to Chemical Weathering of Rock-Forming Minerals

We used the SiB algorithm to relate water compositions to weathering reactions. In brief, the assumption made in this algorithm is that dissolved silica and bicarbonate are exclusively produced by chemical weathering of the dominant primary minerals into secondary (clays) minerals. The other major anions are considered to have come from atmospheric and anthropogenic sources. Knowing the principal primary rock-forming minerals in the area and their most likely weathering products, the SiB algorithm uses stoichiometries of the weathering reactions to relate the chemistries of groups of water, as identified using the RST algorithm, to the contributions of water-rock interactions as well as of other sources. In this manner we can make quantitative estimates of the contributions made by water-mineral reactions and other sources to the water compositions.

Results and Discussion

Figure 3 shows the distribution of a set of 160 samples collected from springs and fresh wells in the Fundão area. The chemical composition of the water samples is given in Table 6. This information was compiled from *Van der Weijden et al.* [1983].

Results of the RST Algorithm

The results of the procedure followed to find groups of water samples with similar chemistries using the RST algorithm are summarized in Table 7. Groups 1 to 10 of Table 7 (equivalence classes with five or more samples) will be considered further. These groups represent 72% of the population. The remaining samples are classified either as anomalies, because they have abnormally high concentrations in one or more of the ions (12% of the population), or as scattered samples, because they do not show any remarkable characteristic (16%). The anom-

Table 6. Data Set

Nr	T	Na^+	K^+	Mg^{2+}	Ca^{2+}	Cl^-	SO_4^{2-}	NO_3^-	HCO_3^-	$H_2SiO_3^o$
28	3	613	39	245	433	447	178	371	780	656
30	3	691	38	242	468	493	229	460	844	639
31	2	613	15	129	315	430	93	387	490	506
32	3	491	31	100	260	287	65	371	390	558
35	3	639	25	183	320	353	171	221	729	614
39	2	406	17	121	128	235	65	216	620	260
41	3	332	19	74	180	192	99	55	261	463
42	3	396	8	58	8	132	63	139	370	421
45	2	1070	55	387	488	680	232	121	1280	571
51	2	817	36	275	650	508	229	189	780	100
59	2	1683	52	683	1142	2152	318	150	2260	674
60	3	433	13	126	217	252	79	63	561	524
61	3	439	11	93	158	235	42	18	580	560
63	2	704	76	300	622	803	367	998	229	399
66	3	530	7	192	325	301	162	366	480	474
67	3	591	9	129	236	247	2	$\gg 0$	1052	684
71	3	470	16	192	199	186	217	5	639	626
72	3	330	6	19	13	166	28	1	239	478
74	3	424	14	80	146	152	22	32	661	609
75	2	313	7	105	88	141	31	1	480	399
76	2	374	11	150	200	158	46	5	810	503
77	3	792	20	204	405	560	119	258	851	499
78	2	1796	197	400	630	1693	236	875	918	438
79	3	407	11	113	136	184	63	121	410	634
84	3	509	7	171	221	313	161	211	451	426
85	3	425	9	88	221	172	47	82	590	606
86	3	570	25	183	200	284	18	60	870	663
87	3	470	2	92	123	247	89	1	451	613
90	3	535	11	150	181	252	63	47	761	506
92	2	452	14	92	145	189	58	$\gg 0$	580	552
96	2	591	11	75	73	341	29	32	480	652
99	2	752	21	171	248	577	183	37	600	353
202	2	856	43	419	708	1320	654	840	139	573
203	2	677	25	196	272	379	209	185	610	440
204	2	527	11	114	126	258	865	158	352	657
205	2	748	23	296	375	545	202	380	716	485
206	2	731	21	156	207	689	145	37	472	441
207	2	708	13	236	422	631	238	500	244	489
208	3	433	11	75	88	184	86	92	328	474
209	2	567	21	107	213	235	161	240	367	532
210	3	362	11	45	75	186	38	82	389	626
211	2	716	69	232	381	402	192	71	1080	587
212	3	397	27	70	130	86	86	143	357	603
213	2	830	32	337	556	703	216	855	429	405
214	3	528	11	112	229	224	219	203	215	437
215	3	457	345	125	170	123	87	18	690	564
216	3	518	14	213	356	192	113	53	1113	660
217	3	541	11	90	225	247	45	3	787	654
218	2	604	88	302	1306	493	114	181	2995	635
219	3	710	53	238	457	775	69	877	167	465
220	2	1968	155	2163	1133	2524	524	1081	3656	264
221	2	495	11	94	139	212	68	3	477	522
222	3	538	23	172	285	264	97	216	642	634
223	3	530	11	218	308	258	185	435	326	485
224	3	359	57	162	386	132	69	77	1156	411
225	3	393	15	71	155	135	113	58	372	472
226	2	387	16	132	66	114	79	85	436	545
227	3	409	27	80	186	126	77	226	367	581
228	3	667	41	201	328	272	171	177	836	750
229	3	880	40	140	230	545	81	205	557	666
230	3	666	11	136	210	206	159	21	664	546
231	3	592	15	127	330	181	224	124	626	508
232	2	565	33	75	213	178	40	435	334	745
233	2	1227	82	603	1165	803	257	2903	690	687
234	3	443	11	89	215	161	139	132	433	670
235	3	473	25	43	147	158	35	65	523	668
236	2	1265	74	503	1192	1377	572	1387	602	586
237	3	427	12	74	154	120	48	248	400	207
238	3	403	11	68	109	143	68	68	438	535
239	3	633	62	219	392	330	137	500	600	558
241	3	256	12	33	41	80	12	61	231	514
242	3	215	11	9	22	66	5	71	136	445

Table 6. (continued)

Nr	T	Na^+	K^+	Mg^{2+}	Ca^{2+}	Cl^-	SO_4^{2-}	NO_3^-	HCO_3^-	$H_2SiO_3^o$
243	2	1097	109	486	763	890	258	435	1529	776
244	3	656	18	105	254	270	168	250	323	476
245	2	536	29	153	265	316	87	131	692	608
246	3	493	11	99	170	129	76	131	564	519
247	3	593	13	125	269	287	186	167	454	532
248	2	656	24	196	347	198	192	500	526	415
249	3	418	12	83	83	109	85	52	408	560
250	3	711	31	163	124	273	139	324	187	579
251	3	316	16	15	24	95	8	35	203	467
252	3	283	11	12	23	106	3	66	128	414
253	2	356	11	24	31	92	33	61	249	619
254	3	345	16	69	45	118	37	29	296	600
255	3	383	11	66	47	126	36	66	293	672
256	3	385	11	38	32	132	38	35	236	520
257	3	474	11	72	60	146	50	140	243	613
258	3	184	11	12	14	98	5	66	59	237
259	3	635	29	210	234	267	87	190	723	740
260	3	481	12	102	140	143	31	43	648	760
261	2	1177	93	296	517	947	183	452	675	620
262	2	2312	113	700	1254	3385	375	1516	1048	617
263	2	1846	93	1051	1827	3213	725	1241	1724	740
264	3	549	16	114	252	338	102	250	451	550
265	3	407	11	59	90	155	22	9	567	697
266	2	1123	36	586	1018	1320	892	532	1278	486
267	2	938	46	294	78	574	56	182	1278	739
268	2	740	27	231	377	537	220	282	526	581
269	2	3889	193	663	1794	6886	559	1048	877	567
270	2	1016	55	799	855	1348	338	726	1169	452
271	3	481	18	72	856	218	25	139	449	842
272	3	365	26	85	126	264	6	187	367	573
273	3	359	19	65	144	166	12	4	554	723
274	3	492	11	108	105	310	52	150	470	530
275	3	417	27	89	107	287	13	105	516	662
276	3	547	15	135	223	488	35	176	531	615
277	3	447	49	143	191	367	59	113	606	736
278	3	359	11	54	75	207	18	113	375	760
279	3	690	22	158	212	602	67	118	688	692
280	3	271	43	43	90	155	11	13	434	583
402	3	165	24	25	34	116	7	22	150	211
404	3	266	24	43	105	192	10	32	308	399
406	3	987	33	127	195	634	75	60	853	692
407	2	1152	67	446	676	757	200	106	2081	757
408	3	430	34	181	76	273	70	112	551	711
410	3	290	27	78	47	109	12	74	272	530
411	2	177	48	122	75	202	46	30	214	209
415	3	465	6	115	42	248	17	8	470	612
420	3	313	15	53	108	213	23	14	390	340
421	3	317	31	70	97	192	22	23	353	339
423	3	241	18	93	29	89	16	29	262	352
424	3	468	26	78	119	236	39	81	365	445
425	3	375	32	115	183	92	10	11	819	812
427	3	354	38	61	101	165	5	30	433	534
430	3	645	29	89	302	245	162	34	725	464
432	3	368	39	43	57	164	9	25	338	689
433	3	327	11	59	64	108	41	24	280	524
434	3	239	31	48	52	80	8	13	292	524
435	3	293	38	39	67	65	5	5	421	581
438	2	454	47	68	57	155	30	30	430	487
439	3	448	55	68	134	130	13	$\gg 0$	714	709
440	3	398	36	68	134	129	29	7	636	729
441	3	472	47	129	237	172	33	8	957	875
442	3	680	58	166	283	846	25	75	607	838
443	3	475	45	156	147	384	33	33	549	569
444	3	301	38	95	60	160	13	36	351	442
446	3	488	34	102	171	260	14	33	651	887
447	2	707	72	207	373	542	95	107	974	548
452	3	669	50	198	332	344	176	105	838	774
453	3	607	36	197	253	280	46	17	1124	752
457	3	304	36	62	146	94	1	1	566	568
458	3	330	35	66	148	196	9	22	526	670
463	2	313	37	71	82	245	33	31	231	366
514	2	371	31	96	188	164	66	27	558	497
522	2	442	30	241	294	184	47	32	1150	600

Table 6. (continued)

Nr	T	Na^+	K^+	Mg^{2+}	Ca^{2+}	Cl^-	SO_4^{2-}	NO_3^-	HCO_3^-	$H_2SiO_3^o$
523	2	600	39	118	282	307	149	34	650	860
524	2	576	63	145	293	252	114	21	919	679
525	2	400	47	86	142	128	69	48	503	554
530	2	669	37	168	316	462	178	62	643	742
534	2	471	36	95	150	281	81	100	310	604
535	2	548	113	245	404	737	143	105	625	568
536	2	370	41	99	254	240	55	42	529	431
539	2	566	51	100	289	697	113	150	600	375
540	2	319	84	124	186	228	23	63	520	806
573	2	177	35	28	29	199	10	19	96	280
574	3	634	80	223	241	930	95	29	652	515
575	2	596	81	223	224	433	130	30	876	514
583	2	880	166	738	452	2390	134	284	305	415
589	3	302	88	121	146	208	19	24	502	679
591	2	450	134	183	285	419	209	20	572	228

Chemical analyses (in μM) of 160 water samples from the Fundão area. The sample numbers are given in the first column; their locations are shown in Figure 3. In the second column (T) the type of sampled water is given: 2, fresh wells; 3, springs.

alies were divided into two groups, one containing the anomalies in HCO_3^-, and the other containing highly polluted samples (enriched in SO_4^{2-} and/or Cl^- and/or NO_3^-).

Weathering Reactions Considered in the SiB Algorithm

The SiB algorithm was applied to water groups 1 to 10 (Table 7). The weathering reactions used in the calculations were the ones from the weathering models already defined for the plutonite and for the dikes (Tables 5a and 5b). The assumed structural formulas of the primary minerals present in these rocks and of the secondary minerals formed upon chemical weathering are given in Table 8. The extreme weathering reactions (the ones that form just one weathering product) for the plutonite and for the amphibolites are listed in Table 9. The results of the analysis of the water-rock interactions are presented in Table 10.

Possible and Best-Fit Solutions of the SiB Algorithm

No information is available about the relative abundances of the secondary minerals in the soils that have developed on the various rocks in the area. For this reason the SiB algorithm (Appendix 2) can generate only sets of possible solutions. We used information about the chemistry of the locally applied fertilizers to find a best-fit solution among the possible solutions. Chloride, sulphate, and nitrate are the major anionic constituents while calcium is a major cationic constituent of these fertilizers. As a best-fit solution among the possible solutions, we selected the one with the most significant Spearman rank-order correlation coefficient between the sum of these anions (in microequivalents per liter) and Ca (in microequivalents per liter). For the best-fit solution high correlation coefficients are also expected for Mg (fertilizers) and Na (mainly domestic effluents) because these cations are not taken up by plants as effectively as K.

Results of the SiB Algorithm

The best-fit weathering reactions, relating the water chemistries to the various rocks, are given in the third row of Table 10. For groups 6 and 10 these reactions are combinations of end-member reactions.

Figure 4 shows the correlation between the median concentrations of Ca^{2+}, Mg^{2+}, and Na^+ attributed to pollution (denoted by a "p" in Table 10, left-hand column) of groups 1 to 6 and 8 to 10 and the sum of the medium concentrations of Cl^-, SO_4^{2-}, and NO_3^-. The corresponding Spearman coefficients are 0.90, 0.95, and 0.92 for probability levels of 99.991%, 99.999%,

Table 7. Groups Obtained by the Equivalence-Classes Procedure

Designation	Sample Numbers	*n*	% gr	% cum
1	61, 74, 75, 85, 92, 235, 246, 260, 265, 273, 275, 415, 440, 443, 446, 457, 458, 514, 525, 536, 540, 589	22	14	14
2	41, 72, 241, 242, 251, 252, 253, 254, 255, 256, 257, 402, 404, 410, 411, 423, 433, 434, 463, 573	20	13	27
3	87, 96, 221, 225, 238, 249, 280, 420, 421, 427, 432, 435, 438, 444	14	9	36
4	42, 79, 204, 208, 210, 212, 226, 227, 237, 271, 272, 278, 424, 534	14	9	45
5	35, 203, 228, 230, 231, 259, 430, 452, 523, 530	10	6	51
6	67, 211, 216, 224, 267, 447, 453, 522	8	5	56
7	76, 86, 90, 217, 425, 441, 524, 575	8	5	61
8	31, 32, 66, 223, 232, 239, 248	7	4	65
9	39, 60, 222, 245, 276, 277, 408	7	4	69
10	28, 30, 51, 77, 205	5	3	72
Anomalies (HCO_3^-)	45, 59, 218, 220, 243, 407	6	4	76
Anomalies (pollutants)	63, 78, 202, 213, 219, 233, 236, 262, 263, 266, 269, 270, 583	13	8	84
Scattered samples	71, 84, 99, 206, 207, 209, 214, 215, 229, 234, 244, 247, 250, 258, 261, 264, 268, 274, 279, 406, 439, 442, 535, 539, 574, 591	26	16	100

Here *n* is number of samples per group; % gr, percentage of samples in each group relative to the total number of samples; % cum, cumulative percentage of the samples relative to the total number of samples in the given order of the groups.

Table 8. Simplified Structural Compositions of the Primary Minerals Present in the Major Lithological Units and in Dikes

Mineral	Chemical Formula*
Albite (An 7)	$0.465\ Na_2O \cdot 0.07\ CaO \cdot 0.535\ Al_2O_3 \cdot 2.93\ SiO_2$
Oligoclase (An 20)	$0.4\ Na_2O \cdot 0.2\ CaO \cdot 0.6\ Al_2O_3 \cdot 2.8\ SiO_2$
Oligoclase/andesine (An 30)	$0.35\ Na_2O \cdot 0.3\ CaO \cdot 0.65\ Al_2O_3 \cdot 2.7\ SiO_2$
Andesine (An 35)	$0.325\ Na_2O \cdot 0.35\ CaO \cdot 0.675\ Al_2O_3 \cdot 2.65\ SiO_2$
Andesine (An 40)	$0.3\ Na_2O \cdot 0.4\ CaO \cdot 0.7\ Al_2O_3 \cdot 2.6\ SiO_2$
Labradorite (An 60)	$0.2\ Na_2O \cdot 0.6\ CaO \cdot 0.8\ Al_2O_3 \cdot 2.4\ SiO_2$
Biotite	$0.1\ Na_2O \cdot 0.9\ K_2O \cdot 2\ MgO \cdot 2.1\ FeO \cdot 0.2\ Fe_2O_3 \cdot 0.3\ TiO_2 \cdot 1.5\ Al_2O_3 \cdot 5.9\ SiO_2$
Hornblende	$0.15\ Na_2O \cdot 2.8\ MgO \cdot 2\ CaO \cdot 1.4\ FeO \cdot 0.2\ Fe_2O_3 \cdot 0.75\ Al_2O_3 \cdot 6.9\ SiO_2$
Augite	$0.7\ MgO \cdot 0.8\ CaO \cdot 0.3\ FeO \cdot 0.15\ Al_2O_3 \cdot 1.9\ SiO_2$
Halloysite	$Al_2O_3 \cdot 2\ SiO_2$
Ca-montmorillonite	$CaO \cdot 7\ Al_2O_3 \cdot 22\ SiO_2$
MgCa-montmorillonite	$0.7\ MgO \cdot 0.35\ CaO \cdot 1.65\ Al_2O_3 \cdot 8\ SiO_2$
Vermiculite	$5.5\ MgO \cdot 0.325\ Fe_2O_3 \cdot 1.5\ Al_2O_3 \cdot 5.6\ SiO_2$
Chlorite	$3.5\ MgO \cdot 1.5\ FeO \cdot Al_2O_3 \cdot 3\ SiO_2$

Biotite composition derived from the chemical analyses given in Table 4. The other mineral compositions, partly simplified, are as given by *Deer et al.* [1962].

*Simplified, structural water omitted.

and 99.995%, respectively. We fitted the data plotted in Figure 4 to a straight line using the mean absolute deviation minimizing method [*Press et al.*, 1989], and we found the following relations:

$$[Ca]_p = -72.8 + 0.38 \times \text{pollution}$$

$$[Mg]_p = 81.4 + 0.3 \times \text{pollution}$$

$$[Na]_p = 11.9 + 0.32 \times \text{pollution}$$

where pollution $\equiv [Cl^-] + [SO_4^{2-}] + [NO_3^-]$ (all concentrations in microequivalents per liter).

The slopes of these lines (0.38, 0.30, and 0.32, respectively) represent the rates at which the $[X]_p$ concentrations increase. The high rate of increase of $[Na]_p$ might be the result of contributions of domestic sewage and/or ion exchange reactions occurring in the soil in which Ca and Mg replace Na at exchange sites. The latter would mean that our working hypothesis of a steady state between the occupancy of the exchange sites and the supply of cations in fertilizers is not fully warranted. Table 10 contains the median values of the measured concentrations and of the calculated concentrations attributed to weathering or pollution for all dissolved components. The appearance of negative values indicates that the component was used from the solution and incorporated in the secondary mineral. The predicted relative abundances of the clay minerals as well as the relative contribution of the weathering of plagioclase to the water composition are given in the bottom of Table 10.

General Interpretation of SiB Results

The halloysite abundance predicted by the best-fit solutions presented in Table 10 (bottom) is very high for groups 2, 3, 4, 1, 8, 9, and 5 (close to 100%). For group 6 and group 10, waters with a mixture of halloysite and montmorillonite, rich in halloysite, is predicted as a result of the weathering of plagioclase. This mixture is produced by the combined reaction 0.9(R5) + 0.1(R6) (Table 10). In order to explain the chemistry of

Table 9. Extreme Weathering Reactions for Primary Minerals Given in Table 8

Reaction	Mineral	Weathering Reaction*
(R1)	albite (An 7)	$1.87\ \text{plagioclase} + x\ H_2O + 2\ CO_2 \rightarrow \text{halloysite} + 1.74\ Na^+ + 0.13\ Ca^{2+} + 2\ HCO_3^- + 3.48\ H_2SiO_3^o$
(R2)	oligoclase (An 20)	$1.67\ \text{plagioclase} + x\ H_2O + 2\ CO_2 \rightarrow \text{halloysite} + 1.33\ Na^+ + 0.33\ Ca^{2+} + 2\ HCO_3^- + 2.67\ H_2SiO_3^o$
(R3)	olig./andesine (An 30)	$1.54\ \text{plagioclase} + x\ H_2O + 2CO_2 \rightarrow \text{halloysite} + 1.08\ Na^+ + 0.46\ Ca^{2+} + 2\ HCO_3^- + 2.15\ H_2SiO_3^o$
(R4)	andesine (An 35)	$1.48\ \text{plagioclase} + x\ H_2O + 2\ CO_2 \rightarrow \text{halloysite} + 0.96\ Na^+ + 0.52\ Ca^{2+} + 2\ HCO_3^- + 1.93\ H_2SiO_3^o$
(R5)	andesine (An 40)	$1.43\ \text{plagioclase} + x\ H_2O + 2\ CO_2 \rightarrow \text{halloysite} + 0.86\ Na^+ + 0.57\ Ca^{2+} + 2\ HCO_3^- + 1.71\ H_2SiO_3^o$
(R6)	andesine (An 40)	$2.36\ \text{plagioclase} + x\ H_2O + 1.2\ CO_2 + 0.7\ Mg^{2+} + 1.87\ H_2SiO_3^o \rightarrow \text{MgCa-montmorillonite} + 1.41\ Na^+ + 0.59\ Ca^{2+} + 1.2\ HCO_3^-$
(R7)	biotite	$0.67\ \text{biotite} + x\ H_2O + 4\ CO_2 + 0.35\ O_2 \rightarrow \text{halloysite} + 0.84\ Fe_2O_3 + 0.2\ TiO_2 + 0.13\ Na^+ + 1.2\ K^+ + 1.33\ Mg^{2+} + 4\ HCO_3^- + 1.93\ H_2SiO_3^o$
(R8)	biotite	$\text{biotite} + x\ H_2O + 5\ HCO_3^- + 3.5\ Mg^{2+} + 0.53\ O_2 \rightarrow \text{vermiculite} + 0.93\ Fe_2O_3 + 0.3\ TiO_2 + 0.2\ Na^+ + 1.8\ K^+ + 5\ CO_2 + 0.3\ H_2SiO_3^o$
(R9)	hornblende	$1.33\ \text{hornblende} + x\ H_2O + 6.2\ CO_2 + 0.29\ O_2 \rightarrow \text{chlorite} + 0.77\ Fe_2O_3 + 0.4\ Na^+ + 0.23\ Mg^{2+} + 2.67\ Ca^{2+} + 6.2\ HCO_3^- + 6.2\ H_2SiO_3^o$
(R10)	hornblende	$2.2\ \text{hornblende} + x\ H_2O + 19.68\ CO_2 + 0.77\ O_2 \rightarrow \text{MgCa-montmorillonite} + 1.98\ Fe_2O_3 + 0.66\ Na^+ + 5.46\ Mg^{2+} + 4.05\ Ca^{2+} + 19.68\ HCO_3^- + 7.18\ H_2SiO_3^o$

*Round-off coefficients.

Table 10. Results Obtained With the SiB Algorithm

	Unit								
	γ_5, γ_8	$\gamma\Delta_3$			Δ_{0-2}			Amphibolites and Metadiabases	
Water group	2	3	4	1	8	9	5	10	6
Weathering reaction(s)	(R1)	(R2), (R7)	(R2), (R8)	(R3), (R8)	(R4), (R8)	(R4), (R7)	(R5), (R7)	0.9(R5) + 0.1(R6), (R10)	0.9(R5) + 0.1(R6), (R10)
$[Na^+]1$	236	250	294	305	252	305	336	302	299
$[Na^+]2$	0	2	2	0	1	2	1	3	17
$[Na^+]_p$	65	129	123	117	312	169	319	443	284
$[K^+]1$	0	0	0	0	0	0	0	0	0
$[K^+]2$	0	18	19	1	10	15	6	0	0
$[K^+]_p$	17	6	8	31	15	14	24	36	41
$[Mg^{2+}]1$	0	0	0	0	0	0	0	−46	−46
$[Mg^{2+}]2$	0	39	−73	−5	−37	33	13	54	278
$[Mg^{2+}]_p$	90	99	223	192	416	269	334	496	192
$[Ca^{2+}]1$	36	125	147	262	271	328	448	380	376
$[Ca^{2+}]2$	0	0	0	0	0	0	0	40	206
$[Ca^{2+}]_p$	44	67	109	30	357	105	168	443	100
$\Sigma[X]_r$	272	434	389	563	497	683	804	733	1130
$\Sigma[X]_p$	216	301	463	370	1100	557	845	1418	617
$[B]_t$	252	433	382	579	497	606	720	844	1135
$[Cl^-]_t$	131	173	192	178	304	299	326	553	266
$[SO_4^{2-}]_t$	56	71	136	79	326	140	367	422	136
$[NO_3^-]_t$	51	44	140	53	472	153	150	385	78
Pollution	238	288	468	310	1102	592	843	1360	480
Err$R$(%)	3.8	0.1	0.9	−1.4	0.0	6.0	5.4	−7.0	−0.2
Err$P$(%)	−4.8	2.2	−0.5	8.8	−0.1	−3.0	0.2	2.1	12.5
$[Si]_t$	472	534	591	610	506	615	676	498	629
$[B]_t/[Si]_t$	0.53	0.81	0.65	0.95	0.98	0.99	1.07	1.69	1.80
Halloysite, %	100.0	100	95.5	99.7	98.0	100.0	100	88.7	83.5
Vermiculite, %	...	0.0	4.5	0.3	2.0	0.0	0.0	...	...
Chlorite, %	...	...	...	...	...	...	...	0.0	0.0
MgCa-mon., %	...	...	...	...	...	...	...	11.3	16.5
Plagioclase, %	100.0	96.9	97.3	99.8	98.6	98.3	98.2	97.9	89.9

The groups analyzed were groups 1 to 10. The chemistry of groups 1, 2, 3, 4, 5, 6, 8, 9, and 10 can be explained using the SiB algorithm. The reactions valid for each group are presented in the third row; for groups 6 and 10 they are combined reactions of the extreme reactions given in Table 9. Here [ ] = concentrations of the dissolved components in microequivalents per liter for cations and anions, and in micromoles per liter for dissolved silica; t, total; r, chemical weathering; p, pollution; 1 and 2, derived from weathering of the first and second primary mineral, respectively; $X = Na^+, K^+, Mg^{2+}, Ca^{2+}$. Pollution = $[Cl^-]_t + [SO_4^{2-}]_t + [NO_3^-]_t$. Err$R$(%) and Err$P$(%) are the relative deviations in the charge balances for bicarbonate (Err$R$) and pollution (Err$P$) calculated using (29) and (30), in Appendix 2.

groundwaters, *Garrels* [1967] also suggests that plagioclase alters to similar mixtures of secondary minerals.

Garrels [1967] used a plot of the $[B]_t/[Si]_t$ (mole ratio) versus $[B]_t$ (milligrams per liter) to discriminate between waters related to different types of igneous rocks. In such plot groups 1, 2, 3, 4, 5, 8, and 9 are indeed characteristic of granitoid rocks, whereas groups 6 and 10 are characteristic of andesitic rocks.

Detailed Interpretation of SiB Results

In the following discussion we refer to the petrological information given in Figures 2a and 2b. On the basis of their chemical compositions (Table 1) we calculated An = 3 for the plagioclase in the γ_5 granite and An = 7 for the γ_8 granite. The composition of group 2 waters can be largely explained by chemical weathering of plagioclase (R1) in these rocks. Group 3 waters obtained their composition by a combination of weathering of plagioclase (R2) and biotite (R7) to halloysite.

According to *Costa et al.* [1971] the plagioclases in the Δ_{0-2} granitoids are strongly zonated (An 18 to An 37). On the basis of the CIPW results (Table 3) the average anorthite contents indicate a spatial range from An 8 to An 45 in plagioclases in the Δ_{0-2} units. These changes in the chemical composition of plagioclases are reflected in the chemistries of groups 4, 1, 8, 9, and 5. Group 4 waters are related to chemical weathering (R2) of oligoclase (An 20), group 1 waters to chemical weathering (R3) of oligoclase/andesine (An 30), group 8 and group 9 waters to chemical weathering (R4) of andesine (An 35), and group 5 waters to chemical weathering (R5) of andesine (An 40). For the groups related to rocks with more sodic plagioclase types (groups 1 and 4) biotite weathering leads to the formation of vermiculite (R8); for groups 9 and 5 biotite alters to halloysite (R7). Group 8 and group 9 waters are derived from weathering of the same plagioclase type, but group 8 waters are obviously more polluted, probably resulting in the production of vermiculite. Group 6 and group 10 waters, although collected in the central area, cannot be explained by a combination of the reactions (R2)–(R4) and (R7) and (R8). Instead, the chemistries of these groups can be explained by weathering of andesine (R5) + (R6) and of hornblende (R10). This means that these chemistries are related to the weathering of basic rocks present as dikes in the central area.

Areal Distribution of the Groups

The areal distribution of the waters of groups 2, 3, 4, 1, 8, 9, and 5 is shown in Figure 5a. The distribution coincides rather well with the different petrological units (cf. Figures 2a and 2b). This is additional confirmation of the validity of the results. However, there seem to be some discrepancies. The group 2 waters are also present in the outer rim of the pluto-

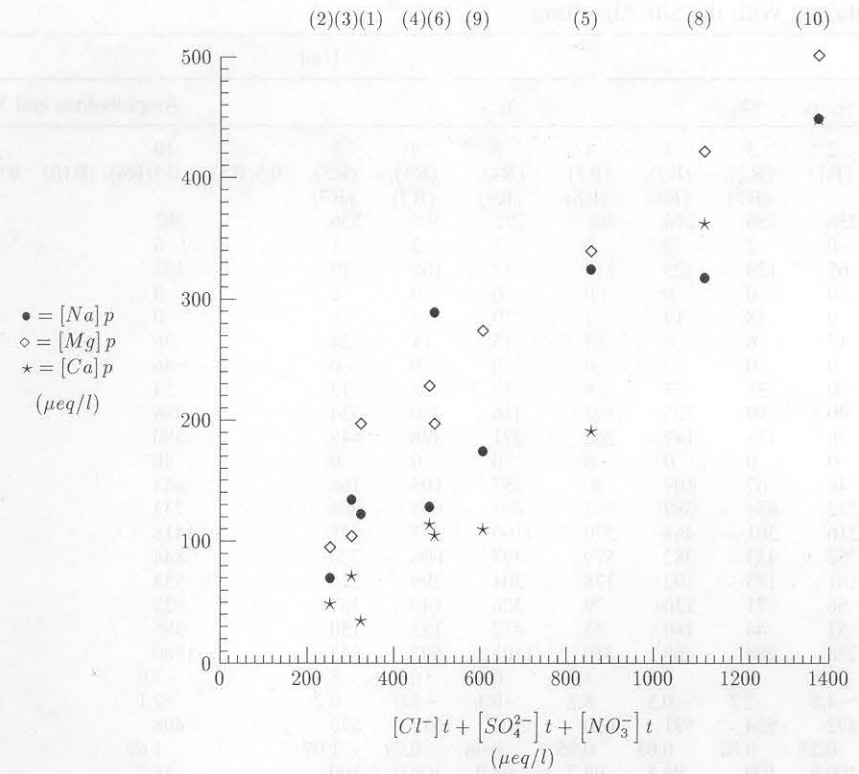

Figure 4. Plot of calculated median Na^+, Mg^{2+}, and Ca^{2+} concentrations attributed to pollution (p) against the sum of the median concentrations of Cl^-, NO_3^-, and SO_4^{2-}. The numbers of the groups are shown in brackets at the top of this figure.

nite, between Fatela and Alcaide and southwest of Alcaide. We believe that these waters acquired their composition by interaction with schists, which is also suggested by the presence of a group 2 type of water near Souto da Casa, situated in schist terrain. Typically, group 2 waters are low in the $[Ca]_r/[Na]_r$ ratio, which is characteristic for the weatherable mineral content of the schists. Another discrepancy is the presence of group 3 waters in the central plutonite. Note, however, that group 3 waters reflect rather intense chemical weathering (biotite → halloysite) of oligoclase-containing granitoids. This is also possible in the central plutonite where composition of the zonated plagioclases varies from oligoclase to andesine and where the presence of dikes may permit deeper infiltration of meteoric water and/or a change in the lateral flow. Within the central area it is not possible to recognize any specific area for groups 4, 1, 8, 9, and 5. This is consistent with the variability of the anorthite content of zonated plagioclase crystals.

The areal distribution of waters in groups 6 and 10 is shown in Figure 5b. It would be too optimistic to expect all sample locations to coincide exactly with the dikes shown on this map, but the figure does support a spatial relation between these waters and the dikes.

It is remarkable that we apparently could explain the water chemistries without taking into account lateral transport of groundwater. One would expect the composition of water that moves laterally from one petrological unit to another to retain and not to lose its inherited signature. It seems, however, that the overprint of the water-rock interactions in the new petrological environment is sufficiently strong to determine the water composition.

Errors

Ideally, when the median concentrations of the groups are expressed in the microequivalents per liter scale, $\Sigma[X]_r = [B]_t$ and $\Sigma[X]_p = [Cl^-] + [SO_4^{2-}] + [NO_3^-]$. Err$R$ and Err$P$ (in percent) (Table 10) are measures of the deviations from ideality. These deviations increase when there are deviations from electroneutrality in the dataset and/or when the medians are not the best estimators of the average concentrations of the ions within a group. In all cases but one (group 6) the deviations are small and considered to be acceptable given the assumptions that had to be made. One should bear in mind that (1) average compositions of the parent minerals, which, especially in the case of the mafic minerals, may not represent the true compositions of the minerals actually being weathered, and that (2) compositions of the weathering products may not exactly represent the compositions of the minerals actually being formed; this holds especially for the smectites, for there is a lack of data on their abundance in the area and their composition.

Our case is basically not different from any other weathering study: the more one knows about abundances and compositions of primary and secondary minerals, the better one can model the water-rock interactions. In our case the extra complicating factor is the relatively high contribution made by other sources, together called "pollution," which causes a poor signal-to-noise ratio.

Anomalous Samples

In the foregoing we showed that we could distinguish the dominant water-rock interactions in the Fundão area, which is

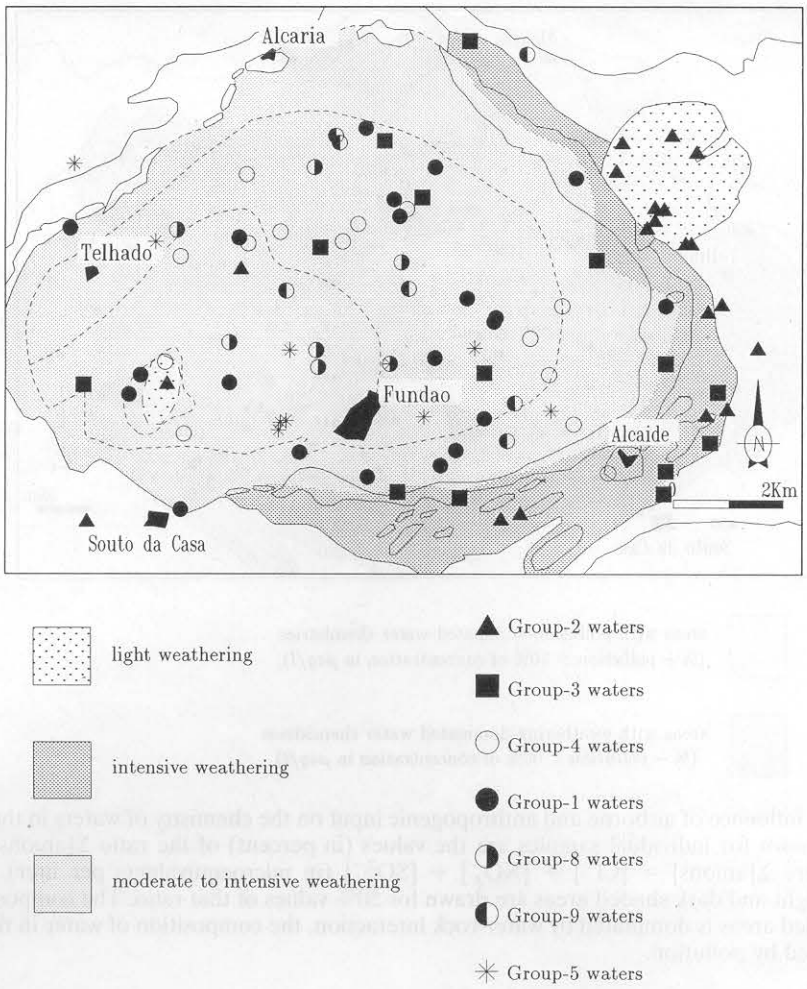

Figure 5a. Waters related to the major rocks in the Fundão area (groups 1 to 5, 8, and 9).

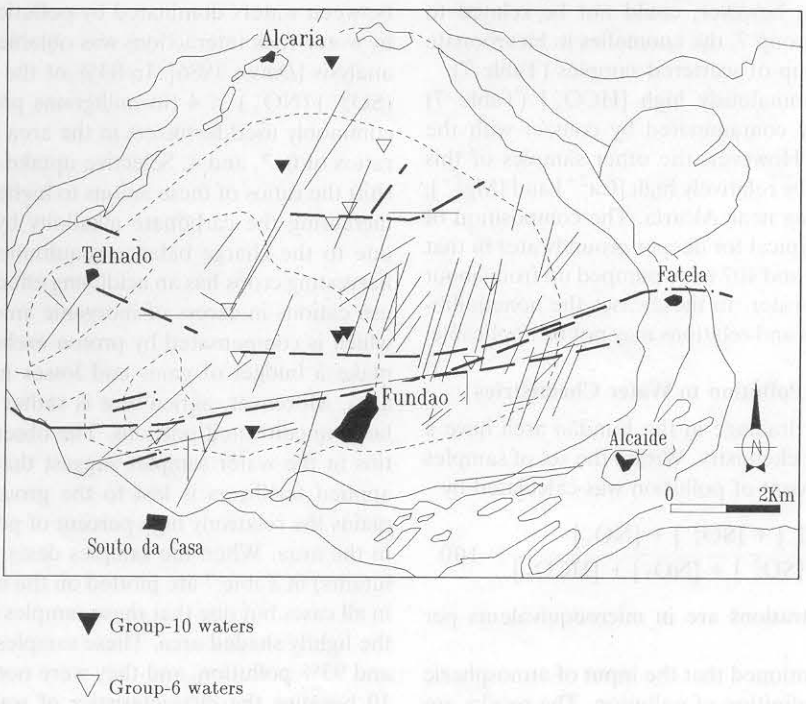

Figure 5b. Waters related to the structures in the Fundão area (groups 6 and 10).

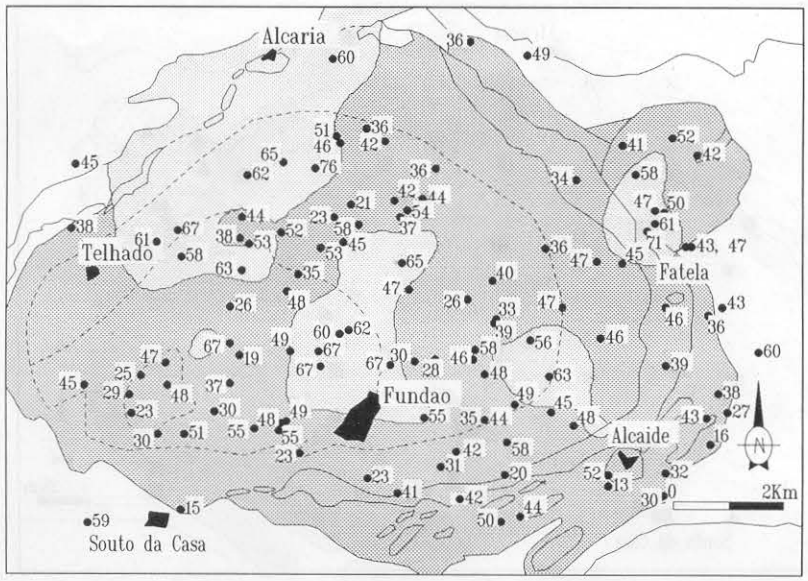

areas with pollution-dominated water chemistries
(% – *pollution* > 50% of concentration in $\mu eq/l$)

areas with weathering-dominated water chemistries
(% – *pollution* < 50% of concentration in $\mu eq/l$)

Figure 6. The influence of airborne and anthropogenic input on the chemistry of waters in the Fundão area. The numbers shown for individual samples are the values (in percent) of the ratio Σ[anions]/(Σ[anions] + [HCO3$^-$]), where Σ[anions] = [Cl$^-$] + [NO_3^-] + [SO_4^{2-}] (in microequivalents per liter). The contours separating the light and dark shaded areas are drawn for 50% values of that ratio. The composition of waters in the dark shaded areas is dominated by water-rock interaction, the composition of water in the light shaded area is dominated by pollution.

complicated with respect to petrology and pollution. Some groups of water samples, however, could not be related to water-rock interactions: group 7, the anomalies in bicarbonate and pollutants, and a group of scattered samples (Table 7).

Of the group with anomalously high [HCO_3^-] (Table 7) sample 218 was probably contaminated by contact with the cement wall of the well. However, the other samples of this group, also characterized by relatively high [Ca^{2+}] and [Mg^{2+}], are from the northern area near Alcaria. The composition of these waters is probably typical for deeper groundwater in that area because samples 220 and 407 were pumped up from about 10 m for use as drinking water. In these cases the nonequilibrium weathering reactions and relations may not be applicable.

Relative Contribution of Pollution to Water Chemistries

Fertilizers and sewage drainage in the Fundão area have a large impact on the water chemistry. Within the set of samples in groups 1 to 10 the percent of pollution was calculated by

$$\% \text{ pollution} = \frac{[Cl^-] + [SO_4^{2-}] + [NO_3^-]}{[Cl^-] + [SO_4^{2-}] + [NO_3^-] + [HCO_3^-]} \times 100$$

where the anion concentrations are in microequivalents per liter.

It has already been mentioned that the input of atmospheric salts is included in this definition of pollution. The results are shown in Figure 6. Contours between light and dark areas represent the 50% pollution values. An identical separation between waters dominated by pollution and those dominated by water-rock interactions was obtained using correspondence analysis [*Davis*, 1986]. In 83% of the 160 water samples $0 < (SO_4^{2-})/(NO_3^-) < 4$ (in milligrams per liter). The three most commonly used fertilizers in the area have SO_4^{2-}/NO_3^- weight ratios of 0, 3, and 4. Selective uptake of NO_3^- by crops would shift the ratios of these anions to higher values, simultaneously increasing the carbonate alkalinity by an equivalent amount due to the charge balance requirement. On the other hand, harvesting crops has an acidifying effect on soils because plants use cations in excess of inorganic anions from the soil water, which is compensated by proton exchange. It is impossible to make a budget of gains and losses in alkalinity in the study area. Moreover, agriculture is rather patchy in an area with large uncultivated portions. The observed sulphate/nitrate ratios in the water samples suggest that a large fraction of the applied fertilizers is lost to the groundwater, which also explains the relatively high percent of pollution in water samples in the area. When the samples designated as anomalies (pollutants) in Table 7 are plotted on the map (Figure 6), one finds in all cases but one that these samples were indeed collected in the lightly shaded area. These samples have scores between 70 and 93% pollution, and they were not included in groups 1 to 10 because the characteristics of water-rock interaction are swamped by the anthropogenic contributions.

Scattered Samples

No attempt has been made to clarify the chemistry of the remaining groups of samples. This would have to be done on a sample-by-sample basis and would require more detailed information about the hydrology than is currently available. Given the purpose of this study, the results are satisfying, since they explain the water chemistries in this complicated area in the great majority of cases.

Conclusions

The RST algorithm that was developed to distinguish groups of water samples with similar chemical characteristics is very effective. The application of the SiB algorithm to relate water compositions of the identified groups to weathering reactions likely to occur in the Fundão area produced promising and mostly convincing results. With the help of this SiB methodology we were able to relate water types with various granitic units in the area and also to basic dikes. This is a remarkable result for an area where anthropogenic contributions to the water chemistry are relatively very high. It should be possible to improve the results when more detailed knowledge is collected about the composition of the primary minerals in the various petrological units, about the abundance and composition of the secondary minerals formed by chemical weathering, and about the field relations between dikes and sites where samples of spring and well waters were collected.

Appendix 1: RST Algorithm

The initial raw data consist of a matrix M_{N_p}, where N is the total number of water samples and p the total number of numerical variables in each water sample. The p variables used in the present case are Na^+, K^+, Mg^{2+}, Ca^{2+}, HCO_3^-, Cl^-, SO_4^{2-}, and NO_3^-.

Stepwise Description of the Algorithm

The RST algorithm comprises three main consecutive steps.

Step 1. The relation between two samples i and j is determined by a measure of similarity, S_{ij}, defined by

$$S_{ij} = 1/(1 + d_{ij}) \tag{1}$$

where

d_{ij} euclidian distance between two points, equal to $[\sum_{k=1}^{p} w_k(M_{ik} - M_{jk})^2]^{1/2}$;
M_{ik}, M_{jk} values for the variable k in samples i and j;
p number of variables;
w_k weight factor of variable k.

Step 2. In this step the S_{ij}'s of each water sample are separated into $S_{ij} = 1$ for the related samples and $S_{ij} = 0$ for the unrelated samples. We adopted the following terminology used in signal processing theory: raw signal, the $N - 1$ S_{ij}'s of each sample sorted in ascending order; noise, a function that describes the values of the S_{ij}'s for the unrelated samples; true signal, the x S_{ij}'s that will be set to $S_{ij} = 1$ (the relevant relations); and filter, the method by which the true signals are separated from the noise. The filtering method consists of the substeps 2.1 to 2.3.

2.1: The $N - 1$ relations are ranked in ascending order of their similarity to i, and this row forms the raw signal of sample i. The sample j in position m on the raw signal is identified as samp_m ($j = \text{samp}_m$).

2.2: The first half of the population (lowest relations) is used to define a noise function:

$$\text{noise}_m = \text{raw signal}_m \qquad \text{if } m \le N/2 \tag{2a}$$

otherwise

$$\text{noise}_m = \text{raw signal}_{N-m} \qquad m = 1, 2, 3, \cdots, N - 1 \tag{2b}$$

It is assumed that at least half of the lowest S_{ij}'s of each sample may not be transformed into relevant relations. By this method no group may have more than $N/2$ elements.

2.3: Now a binary square matrix, the relevant matrix $R_{N\times N}$, can be defined that represents the relevant relations of the samples. The line i of the matrix R (the true signal of sample i) is constructed by setting $R_{ij} \equiv 1$ for a relevant relation between i and j, and $R_{ij} \equiv 0$ otherwise. For computation of the R_{ij}'s the following filter was defined:

$$R_{ij} = \text{nearest integer}\left\{\frac{\text{raw signal}_m - \text{noise}_m}{\text{raw signal}_m}\right\} \tag{3}$$

where $m = 1, 2, 3, \cdots, N - 1$ and $j = \text{samp}_m$.

Step 3. The previous steps do not guarantee the symmetry and transitivity of the relevant relations. The method of selection of the equivalent (symmetric and transitive) relations among the relevant relations identified in the foregoing step is described in the consecutive substeps 3.1 to 3.9.

3.1: The symmetric relations are identified and saved in the elements above the main diagonal of R:

$$R_{ij} = R_{ij} \times R_{ji} \tag{4}$$

where $i = 1, \cdots, N - 1$ and $j = i + 1, \cdots, N$.

3.2: The transitive relations are identified. At the start of the transitivity test all samples have a status $R_{ii} = 1$ (ungrouped). This status changes to $R_{ii} = 0$ when sample i is included in one group. Only the first element of each group remains with its status unaltered.

3.3: To begin a group one looks for a sample i with $R_{ii} = 1$.

3.4: For this sample i one considers the elements j ($j = i + 1, \cdots, N$) with $R_{ij} = 1$.

3.5: For each sample j the value of R_{jj} is tested to check whether j has already been included in another group. If $R_{jj} = 0$ (which means that sample j already belongs to another group), we assign $R_{ij} = 0$ to guarantee that sample j will not be grouped with sample i; otherwise sample j is grouped with sample i; R_{ij} maintains the value 1 and R_{jj} is set to 0. Testing the remaining samples k, one continues to preserve the transitivity between samples i, j, and k by

$$R_{ik} = R_{ik} \times R_{jk} \tag{5}$$

where $k = j + 1, \cdots, N$.

3.6: In case not all samples j with $R_{ij} = 1$ are tested, the procedure starts again at step 3.4.

3.7: The group initiated in step 3.3 is now complete. All samples j of row i with $R_{ij} = 1$ belong to it, and they have $R_{jj} = 0$, whereas $R_{ii} = 1$.

3.8: This procedure must be completed for all samples i which kept $R_{ii} = 1$. Subsequently, another group is initiated, starting with step 3.3, and run until $i = N$.

3.9: The elements of each group are listed. The total number of rows i with $R_{ii} = 1$ defines the number of groups that

have been identified. Each group comprises samples j of the rows with $R_{ij} = 1$.

Additional Remarks

The following remarks regarding this method are due.

1. The transformation of the data by the use of the euclidian distance (step 1) is scale variant, so different results may be obtained when one changes the scale in which the data are expressed. This may seem to reduce the applicability of the method, but the most common partitioning methods all use scale variant measures of similarities or distances to produce the clustering [*Kaufman and Rousseeuw*, 1990].
2. When the number of groups generated in this procedure is quite large, no sample is likely to have more than $N/2$ relevant relations (step 2), in which case no relevant relations are lost.
3. The results of the procedure described in steps 3.3 to 3.8 may, in some cases, depend on the order in which the operations are carried out. This is the case when the data set contains samples that may belong to different but similar groups.

Appendix 2: SiB Algorithm

Stoichiometric Relations

Considering the weathering of a primary silicate mineral M into a combination of two secondary silicates P_1 and P_2, we can write a symbolic reaction:

$$c_M M + \Sigma_c(c_y Y) \rightarrow c_1 P_1 + c_2 P_2 + \Sigma_r(c_y Y) \quad (6)$$

This reaction represents the process by which c_M moles of M are converted into c_1 moles of P_1 and c_2 moles of P_2, $\Sigma_c(c_y Y)$ represents the number of moles of dissolved components consumed by the reaction, and $\Sigma_r(c_y Y)$ the number of moles released. When a component Y is consumed, its source is, in the majority of the cases, weathering of other primary minerals, although Y may also be provided by pollution.

The proportions in which P_1 and P_2 are formed are given by the c_1 and c_2 coefficients. For the use in the SiB algorithm a relation between c_1 and c_2 is established by

$$c_2 = 1 - c_1 \quad (7)$$

where $0 \leq c_1 \leq 1$. The values of the c_M and c_y coefficients are dependent upon the values given to c_1 and c_2 as well as upon the chemical compositions of the primary mineral M and the weathering products P_1 and P_2.

Incongruent Reactions

The major and minor oxides present in the structure of many silicate minerals are Na_2O, K_2O, MgO, CaO, SiO_2, TiO_2, Al_2O_3, Fe_2O_3, FeO, and MnO. The last five oxides are considered to be immobile oxides because their solubility in oxygenated water is very low when compared to the solubility of the first five oxides. The SiB algorithm assumes incongruent weathering, in which all Al_2O_3 is transferred from the structure of the primary minerals to the structure of the weathering products. Similar assumptions were made by *Tardy* [1971].

Calculation of Reaction Coefficients

The conservation of Al_2O_3 in the structure of the minerals can be used to define general equations for the c_M and c_y coefficients.

If $\alpha_{(ox)}m$ is the coefficient of oxide ox in the structural formula of a mineral m (either M or P) then c_M can be calculated by

$$c_M = \frac{c_1\alpha_{(Al_2O_3)}P_1 + c_2\alpha_{(Al_2O_3)}P_2}{\alpha_{(Al_2O_3)}M} \quad (8)$$

where $c_M\alpha_{(Al_2O_3)}M$ represents the number of moles of Al_2O_3 needed to convert c_M moles of M into c_1 moles of P_1 and c_2 moles of P_2 and $\alpha_{(Al_2O_3)}P_1$ and $\alpha_{(Al_2O_3)}P_2$ are the number of moles of Al_2O_3 present in each mole of P_1 and P_2, respectively.

The c_y coefficients are then given by

$$c_{Na} = 2(c_M\alpha_{(Na_2O)}M - c_1\alpha_{(Na_2O)}P_1 - c_2\alpha_{(Na_2O)}P_2) \quad (9)$$

$$c_K = 2(c_M\alpha_{(K_2O)}M - c_1\alpha_{(K_2O)}P_1 - c_2\alpha_{(K_2O)}P_2) \quad (10)$$

$$c_{Mg} = c_M\alpha_{(MgO)}M - c_1\alpha_{(MgO)}P_1 - c_2\alpha_{(MgO)}P_2 \quad (11)$$

$$c_{Ca} = c_M\alpha_{(CaO)}M - c_1\alpha_{(CaO)}P_1 - c_2\alpha_{(CaO)}P_2 \quad (12)$$

$$c_{H_2SiO_3} = c_M\alpha_{(SiO_2)}M - c_1\alpha_{(SiO_2)}P_1 - c_2\alpha_{(SiO_2)}P_2 \quad (13)$$

$$c_{HCO_3} = c_{Na} + c_K + 2c_{Mg} + 2c_{Ca} \quad (14)$$

The equation for the bicarbonate coefficient (equation (14)) balances the symbolic equation for the ionic charge. The signs of these c_y values indicate production or consumption of Y. If a c_y coefficient is negative, then component Y is consumed during the reaction; if c_y is positive, then component Y is released; if $c_y = 0$, then component Y is not involved in the weathering process.

Water Chemistries

The SiB algorithm is based on the assumption that the natural water chemistry may be largely explained by the weathering of one or two silicates. In the case of the weathering of two silicates, M_1 and M_2, the produced concentrations are

$$[HCO_3^-]_t,\ [H_2SiO_3^0]_t,\ [X]_r$$

and the concentrations from pollution are

$$[Cl^-]_t,\ [SO_4^{2-}]_t,\ [NO_3^-]_t,\ [X]_p$$

where $X = Na^+$, K^+, Mg^{2+}, Ca^{2+} and t, r, and p are total, water-rock interaction, and pollution, respectively.

The following equations apply:

$$[X]_r = [X]_1 + [X]_2 \quad (15)$$

$$[X]_p = [X]_t - [X]_r \quad (16)$$

where

- $[X]_t$ molar concentration of X (measured);
- $[X]_r$ molar concentration of X due to weathering;
- $[X]_p$ molar concentration from pollution;
- $[X]_{1,2}$ molar concentrations produced by weathering of minerals M_1 and M_2, respectively.

If we consider the weathering of only one primary mineral, the concentrations with subscript 2 are set to zero.

The purpose of the SiB algorithm is to calculate $[X]_1$, $[X]_2$ and $[X]_p$ for all the cations. The molar mass balance equations for dissolved silica and bicarbonate are

$$r_{Si(M_1)}[M_1] + r_{Si(M_2)}[M_2] = [Si]_t \quad (17)$$

$$r_{B(M_1)}[M_1] + r_{B(M_2)}[M_2] = [B]_t \quad (18)$$

where Si = $H_2SiO_3^o$, B = HCO_3^-, $r_{Si(M)}$ is the ratio between the stoichiometric coefficients of dissolved silica ($c_{H_2SiO_3}$, equation (13)) and of the minerals M (c_M, equation (8)), $r_{B(M)}$ is the ratio between the stoichiometric coefficients of dissolved bicarbonate (c_{HCO_3}, equation (14)) and of the minerals M (c_M, equation (8)), and $[M_1]$, $[M_2]$ is the number of moles of M_1 and M_2 producing $[Si]_t$ and $[B]_t$, given in moles per liter.

Equations (17) and (18) connect the stoichiometric relations of the components, as predicted by the weathering reactions of M_1 and M_2 with the real composition of a given water sample. Writing the previous equations in matrix form we have

$$\begin{bmatrix} r_{Si(M_1)} & r_{Si(M_2)} \\ r_{B(M_1)} & r_{B(M_2)} \end{bmatrix} \begin{bmatrix} [M_1] \\ [M_2] \end{bmatrix} = \begin{bmatrix} [Si]_t \\ [B]_t \end{bmatrix} \quad (19)$$

which can be solved for $[M_1]$ and $[M_2]$.

The concentrations of the cations produced during chemical weathering are then calculated by

$$[X]_1 = r_{X(M_1)}[M_1] \quad (20)$$

$$[X]_2 = r_{X(M_2)}[M_2] \quad (21)$$

where X represents one of the major cations. Then we use (15) and (16) to obtain the concentrations of cations related to pollution.

Solids Consumed and Produced

The percentage to which each mineral is used in the weathering process can be computed by

$$\%\ (M_1) = \frac{[M_1]}{[M_1] + [M_2]} \times 100 \quad (22)$$

$$\%\ (M_2) = 100 - \%(M_1) \quad (23)$$

The number of moles of weathering products can also be calculated:

$$[P_{11}] = r_{c11(M_1)}[M_1] \quad (24a)$$

$$[P_{12}] = r_{c12(M_1)}[M_1] \quad (24b)$$

$$[P_{21}] = r_{c21(M_2)}[M_2] \quad (24c)$$

$$[P_{22}] = r_{c22(M_2)}[M_2] \quad (24d)$$

where $[P_{11}]$, $[P_{12}]$ are the number of moles of P_{11} and P_{12} produced in weathering of $[M_1]$ moles of M_1, $[P_{21}]$, $[P_{22}]$ are number of moles of P_{21} and P_{22} produced in weathering of $[M_2]$ moles of M_2; $r_{c11(M_1)}$, $r_{c22(M_1)}$ are ratios of the stoichiometric coefficients of P_{11} and M_1 and of P_{12} and M_1 (equations (7) and (8)), and $r_{c21(M_2)}$, $r_{c22(M_2)}$ are ratios of the stoichiometric coefficients of P_{21} and M_2 and of P_{22} and M_2 (equations (7) and (8)). The relative abundance of each clay mineral with respect to the other clay minerals may be computed using equations similar to (22) and (23).

The solution is straightforward if chemical weathering affects only one mineral M. We can write the molar mass balance for silica by

$$r_{Si(M)}[M] = [Si]_t \quad (25)$$

which immediately gives

$$[M] = [Si]_t / r_{Si(M)} \quad (26)$$

The other concentrations and mole fractions are then calculated exactly as in the previous situation.

Combining Results Obtained With the RST and SiB Algorithms

In principle, the SiB algorithm can be applied to groups found by other clustering techniques as well. But the success depends on how well the groups represent waters with similar chemistries. The groups identified by the RST algorithm will have similar chemistries. In order to know how these chemistries are related to chemical weathering we have to attribute the average compositions of the groups to envisaged weathering reactions. This is done in the following manner.

1. By using (15), (16), and (19)–(24), we can calculate, for each sample in the group, the natural and pollution-derived concentrations of each cation, the number of moles of the primary and secondary minerals involved in the envisaged weathering reactions, and, in the case of weathering of just one mineral, the charge balance deviations (see equations (29) and (30)).

2. Median values are calculated of each of those concentrations, of each of the number of moles of primary and secondary minerals, and of each of the charge balance deviations. Since medians are robust estimators [*Press et al.*, 1989], these single values are considered to be representative for the whole group.

Additional Criteria

When we apply the SiB algorithm to the median water composition of a group, using a specific set of weathering reactions, we need to test whether or not that group is related to those reactions. The following criteria have to be satisfied simultaneously.

1. With respect to the water composition, first, the natural concentrations of a given component Y must have a positive sign when the weathering reactions predict the release of such component ($c_y > 0$), and they must have a negative sign when consumption of Y is expected during the weathering process ($c_y < 0$). This check is made as follows: after calculation of median $[X]_1$ and $[X]_2$ for all the cations we compare the signs of those values with the signs of the corresponding stoichiometric coefficients c (equations (9)–(12)); if they are equal for all the cations, then the group is related to the predefined set of weathering reactions; otherwise the group has to be tested with an other set of weathering reactions. Second, all the median pollution concentrations must be positive.

2. With respect to the weathering products, the median relative abundances of the weathering products, predicted by the SiB algorithm (equations (24a)–(24d)) should be in agreement with the real abundances in the area in which the water samples were collected. The results cannot often be checked against this criterion because the relative abundances of the weathering products are poorly known or not known at all. In those cases the SiB algorithm is only capable of giving sets of possible results which meet the requirements with respect to the water composition.

3. If we have only one mineral, we will have to satisfy the previous criteria as well as the charge balances. We only use the molar mass balance of dissolved silica (equation (25)), and for that reason the charge balances are not guaranteed. We consider that a given group is related to the weathering of one mineral if the median deviations of the charge balances for bicarbonate and pollution are less than 10% of the total ionic charge. Charge balance equations for bicarbonate and pollution are given by

$$\Sigma z_X[X]_r = [HCO_3^-]_t \quad (27)$$

$$\Sigma z_X[X]_p = [Cl^-]_t + 2[SO_4^{2-}]_t + [NO_3^-]_t \equiv \text{pollution} \quad (28)$$

where z_X is the ionic charge of X. The deviations in the charge balances for bicarbonate (Err$R$) and pollution (Err$P$) are calculated by

$$\text{Err}R(\%) = \frac{\Sigma z_X[X]_r - [HCO_3^-]_t}{\Sigma z_X[X]_r + [HCO_3^-]_t} \times 100 \quad (29)$$

$$\text{Err}P(\%) = \frac{\Sigma z_X[X]_p - \text{pollution}}{\Sigma z_X[X]_p + \text{pollution}} \times 100 \quad (30)$$

Geological criteria may be used. An important clue is that we write each set of weathering reactions with a specific petrological area in mind. In the end the samples related to that set of weathering reactions must have a spatial relation with the petrology and mineralogy of that area.

Acknowledgments. The first author received an ERASMUS scholarship from the European Community upon the recommendation of M. Portugal Ferreira of the Geology Department of the Universidade de Coimbra. He also thanks João Brandão of the Chemistry Department of Coimbra University for his advice. R. D. Gill of the Mathematical Department of Utrecht University gave helpful comments on the RST algorithm presented in this paper. We also thank two anonymous referees and the associate editor for their constructive remarks and suggestions on an earlier version of this paper. Contribution 960501 of the Netherlands Research School of Sedimentary Geology.

References

Costa, C. V., L. G. Pereira, M. Portugal Ferreira, and J. M. Santos Oliveira, Distribuição de oligoelementes nas rochas e solos da região do Fundão, *Memórias e Notícias*, Mus. e Lab. Mineral. e Geol. da Univ. de Coimbra, *71*, 1–37, 1971.

Davis, J. C., *Statistics and Data Analysis in Geology*, 646 pp., John Wiley, New York, 1986.

Deer, W. A., R. A. Howie, and J. Zussmann, *Rock-Forming Minerals*, vol. 1–5, Longmans, Green, Toronto, Ont., 1962.

Drever, J. I., *The Geochemistry of Natural Waters*, 437 pp., Prentice-Hall, Englewood Cliffs, N. J., 1988.

Everitt, B., *Cluster Analysis*, 122 pp., Heinemann, London, 1977.

Garrels, R. M., Genesis of some ground waters from igneous rocks, in *Researches in Geochemistry*, vol. 2, edited by P. H. Abelson, pp. 405–420, John Wiley, New York, 1967.

Garrels, R. M., and F. T. Mackenzie, Origin of the chemical compositions of some springs and lakes, in *Equilibrium Concepts in Natural Water Systems*, *Adv. Chem. Ser.*, vol. 67, edited by R. F. Gould, pp. 222–242, Am. Chem. Soc., Washington, D. C., 1967.

Hartigan, J., *Clustering Algorithms*, 351 pp., Wiley-Interscience, New York, 1975.

Kaufman, L., and P. J. Rousseeuw, *Finding Groups in Data*, 342 pp., John Wiley, New York, 1990.

Pačes, T., Chemical characteristics and equilibration in natural water-felsic rock—CO_2 system, *Geochim. Cosmochim. Acta*, *36*, 217–240, 1972.

Pačes, T., Steady-state kinetics and equilibrium between ground water and granitic rock, *Geochim. Cosmochim. Acta*, *37*, 2641–2663, 1973.

Portugal Ferreira, M., A magmatic arc in the Iberian Segment of the Hercynian chain, I, The northwest-southeastlineament between Oporto (Portugal) and Zarza la Major (Spain), *Memórias e Notícias*, Mus. e Lab. Mineral. e Geol. da Univ. de Coimbra, *94*, 31–50, 1982.

Portugal Ferreira, M., E. Ivo Alves, and C. A. Regêncio Macedo, A zonalidade de um plutonito: estruturas condicionantes e idades de evolução (Plutonito do Fundão, Portugal central), *Memórias e Notícias*, Mus. e Lab. Mineral. e Geol. da Univ. de Coimbra, *99*, 167–186, 1985.

Press, W. H., B. P. Flannery, S. A. Teukolsky, and W. T. Vetterling, *Numerical Recipes in Pascal*, 759 pp., Cambridge Univ. Press, New York, 1989.

Sverdrup, H. V., and P. Warfvinge, On the geochemistry of chemical weathering, in *Chemical Weathering Under Field Conditions*, *Rep. For. Ecol. For. Soil 63*, edited by K. Rosén, pp. 79–119, Swed. Univ. Agric. Sci., Uppsala, 1991.

Tardy, Y., Characterization of the principle weathering types by the geochemistry of waters from some European and African crystalline massifs, *Chem. Geol.*, *7*, 253–271, 1971.

Tardy, Y., G. Bocquier, H. Paquet, and G. Millot, Formation of clay from granite and its distribution in relation to climate and topography, *Geoderma*, *10*, 271–284, 1973.

Van der Weijden, C. H., M. G. Oosterom, J. Bril, C. G. Walen, S. P. Vriend, and B. W. Zuurdeeg, Geochemical controls of transport and deposition of uranium from solution: Case study: Fundão, Portugal, *Tech. Rep.*, Inst. of Earth Sci., Dep. of Geochem., Utrecht Univ., Utrecht, Netherlands, 1983.

Velbel, M. A., Geochemical mass balances and weathering rates in forested watersheds of the southern Blue Ridge, *Am. J. Sci.*, *285*, 904–930, 1985a.

Velbel, M. A., Hydrogeochemical constraints on mass balances in forested watersheds of the southern Appalachians, in *The Chemistry of Weathering*, *NATO ASI Ser.*, edited by J. I. Drever, pp. 231–247, D. Reidel, Norwell, Mass., 1985b.

Velbel, M. A., Weathering of hornblende to ferruginous products by a dissolution-reprecipitation mechanism: Petrography and stoichiometry, *Clays Clay Miner.*, *37*, 515–524, 1989.

Velbel, M. A., Geochemical mass balances and weathering rates in forested watersheds of the southern Blue Ridge, III, Cation budgets and the weathering rate of amphibole, *Am. J. Sci.*, *292*, 58–78, 1992.

F. Pacheco, Secção de Geologia, Universidade de Trás-os-Montes e Alto Douro, 5000 Vila Real, Portugal. (e-mail: fpacheco@utad.pt)

C. H. Van der Weijden, Department of Geochemistry, Institute of Earth Sciences, Utrecht University, P.O. Box 80.021, 3508 TA Utrecht, Netherlands. (e-mail: chvdw@earth.ruu.nl)

(Received January 15, 1996; revised May 28, 1996;
accepted May 28, 1996.)